atmosphere

MDPI

Article

Planning for a Warmer Future: Heat Risk Assessment and Mitigation in Lahti, Finland

Ankur Negi [1,*], Rohinton Emmanuel [1,*] and Eeva Aarrevaara [2]

[1] The Research Centre for Built Environment Asset Management (BEAM), School of Computing, Engineering and the Built Environment, Glasgow Caledonian University, Glasgow G4 0BA, UK
[2] LAB University of Applied Sciences, 15210 Lahti, Finland; eeva.aarrevaara@lab.fi
* Correspondence: anegi300@caledonian.ac.uk (A.N.); rohinton.emmanuel@gcu.ac.uk (R.E.)

Abstract: With global climate change causing temperature increases, even cooler regions like Finland are facing increasing heat risks. The city of Lahti is expected to experience a higher-than-average temperature increase, making heat risk mitigation essential. This study aims to assess present and future heat risks in Lahti using exposure and social vulnerability indicators to identify heat risk hotspots and provide strategies for mitigation within the city's urban planning framework. The method utilizes a combination of Land Surface Temperature (LST) data (2014–2024), climate projections, and microclimate analysis to identify heat risk in the city. Geographic Information Systems (GIS) and ENVI-met modeling were employed to assess the relationship between land surface temperatures (LST), urban structure, and green infrastructure. Risk assessments were conducted using social and environmental vulnerability indicators, and future projections were based on a combined SSP2-4.5 scenario. The results show a significant increase in high-risk areas by 2040, rising from 9.79% to 23.65% of Lahti's core urban area. Although the current urban planning framework of the city (Masterplan 2035) is effective in terms of maintaining exposure levels, the continued increase in projected air temperatures, as modeled based on outputs of the EC-Earth3-veg GCM, remains a concern. Microclimate modeling confirmed that urban greenery significantly reduces heat stress and improves thermal comfort. To address future heat risks, Lahti must integrate more green infrastructure into its urban design and identify seasonal heat mitigation methodologies. Additionally, the findings emphasize the need for adaptive planning strategies to mitigate rising temperatures and ensure urban resilience.

Keywords: heat risk mapping; micro-climate modeling; thermal comfort

check for updates

Academic Editors: Ferdinando Salata and Matthew Eastin

Received: 5 December 2024
Revised: 7 January 2025
Accepted: 25 January 2025
Published: 29 January 2025

Citation: Negi, A.; Emmanuel, R.; Aarrevaara, E. Planning for a Warmer Future: Heat Risk Assessment and Mitigation in Lahti, Finland. *Atmosphere* **2025**, *16*, 146. https://10.3390/atmos16020146

Copyright: © 2025 by the authors. Licensee MDPI, Basel, Switzerland. This article is an open access article distributed under the terms and conditions of the Creative Commons Attribution (CC BY) license (https://creativecommons.org/licenses/by/4.0/).

1. Introduction

In recent years, Europe has experienced an unprecedented rise in extreme heat events, which can be primarily attributed to the impacts of climate change [1]. The summer of 2018 marked the hottest on record, with severe heatwaves across multiple regions in Europe, only for these records to be surpassed in 2019 [2–4]. That year saw historically high temperatures across France, Poland, Germany, Spain, and Switzerland, while the United Kingdom recorded its highest-ever temperatures and broke local records at 46 stations across the country [5]. According to the Intergovernmental Panel on Climate Change (IPCC), climate change has intensified the frequency and severity of these heatwaves, exacerbating heat risks even in traditionally cooler, northern latitude countries [6–10].

Despite its northern location, Finland, lying between 60° and 70° N, experiences warm summers due to its continental climate. Although known for its colder climatic

conditions in the winter, Finnish summer temperatures now frequently exceed 30 °C in most parts of the country [11,12]. A notable extreme occurred in Joensuu in July 2010, where temperatures soared to a record-breaking 37.2 °C [13]. Finland's vulnerability to warming temperature trends has been further demonstrated by the recent heatwaves in May and July 2018 which affected nearly the entire country and resulted in national mean temperature records exceeding prior records by 0.5 °C and 0.4 °C, respectively [14].

From 1991 to 2020, Finland's mean annual temperature increased by approximately 0.6 °C compared to the 1981–2010 period, and by 1.3 °C relative to 1961–1990 [15]. Seasonal analyses indicate that winter months have seen the most notable warming [16]. Climate projections suggest that temperatures will continue to rise significantly, with estimates that by 2050, January and February in Helsinki will be about 2 °C warmer than they were from 1971–2000, and mean March temperatures will likely remain above freezing. By the end of the century, it is expected that all monthly average temperatures will be positive [17].

The rapid warming trend in Finland is significant; studies show that Finland's rate of temperature increase due to global warming is projected to be 1.5 to 2 times faster than the global average [11,18,19]. This susceptibility highlights the serious risks a warming climate poses to Finland's environment, public health, infrastructure, and economy. Extreme heat can particularly affect vulnerable populations, such as the elderly, while also disrupting traditional frost patterns essential for winter activities and altering forestry, agriculture, and hydrological systems [20,21]. If not mitigated, these shifts could trigger a cascade of challenges, including increased heat stress, changes in snowmelt patterns, and a heightened risk of floods [22,23].

Urban areas are particularly susceptible to the increasing temperatures posing challenges to urban climate and thermal comfort [24]. Urban heat islands and associated risks also occur in colder regions like Finland [25]. Ref. [26] found that while temperature variations in winter were primarily driven by atmospheric inversions, the UHI effect was the main driver of temperature differences within Lahti during the summer months. Assessing heat risk and thermal comfort in urban areas thus becomes important to ensure the negative effects of heat on people [24]. Multiple studies utilize the relationship between land surface temperature (LST) and local climate zones (LCZ) to understand the thermal effects of urban morphology highlighting key landcover features that exacerbate UHI [27–30]. Adaptation utilizing green infrastructure is key to reducing these impacts [31,32].

While the general trends in national temperature in Finland are well known, there is a significant gap in our understanding of the localized effects of climate change within the urban environment in Finland, particularly in cities outside the Helsinki urban area. Given the current drive to develop urban climate resilience plans at the municipal level (https://ym.fi/en/-/government-proposal-municipalities-obliged-to-draw-up-climate-plans-in-future, accessed on 26 January 2025) (Climate Change Act, 2022), there is a need to understand the spatial and temporal dimensions of heat risks and identify vulnerable areas, which could help develop a richer urban climate resilience approach. Effective urban adaptation will be critical in minimizing the socioeconomic and environmental impacts of climate change across Finnish cities, particularly as they grapple with intensifying risks and warmer climates.

This study focuses on the city of Lahti, aiming to map and quantify areas of future heat risk, as defined in Materials and Methods, by combining climate projections with the city's future masterplans. Specifically, it aims to (1) assess the current heat risk profile using local heat indicators, (2) identify high-risk zones through comprehensive mapping to evaluate the mitigative potential of Lahti's masterplans, and (3) utilize ENVI-met microclimate modeling to propose effective mitigation strategies for anticipated heat risks. Ultimately,

the research seeks to provide a robust heat risk assessment that can guide Lahti's urban resilience strategies for a warmer future climate.

2. Materials and Methods

The methodology adopted is quantitative, utilizing diverse data sources such as projected mean monthly air temperatures; current mean monthly air temperature; socio-economic and demographic data including population above 65 yrs and below 5 yrs, population density, and employment percentage; satellite and drone imagery-derived data including built-up areas, impervious areas, solar exposure, green areas, and distance from waterbodies; and LiDAR-derived data including digital elevation model and digital surface model, sky view factor, peer-reviewed articles, satellite and drone images, and Geographic Information System (GIS) modeling using a multicriteria decision-making methodology. By focusing on quantifiable, spatial data, the research aims to objectively analyze the current and projected heat risk levels and to evaluate potential urban resilience strategies. Vulnerabilities were quantified using a combination of social, economic, and physical indicators utilizing the Analytical Hierarchy Process (AHP), while heat hazard was derived from past and present Land Surface Temperatures (LST) and EC-Earth3-veg ESM. Additionally, the air temperature data of the Turku Urban Climate Research Group (TURCLIM) of the Geography Section of the University of Turku was utilized in mean monthly air temperature trend analyses and in trend analyses of the summer months (June, July, and August) maximum mean daily temperatures, to assess changes in hazard.

Heat risk was mapped using Crichton's risk triangle framework [33] which defines risk as a function of hazard, vulnerability, and exposure. This study leverages spatial mapping and data analysis techniques to visualize at-risk areas as a product of the hazard, vulnerability, and exposure components of risk, providing critical insights for planners in the city of Lahti and potentially serving as a model for other areas in Finland. Heat risk has been mapped for heatwave days (i.e., very hot days defined by FMI as the maximum daily temperature above 30 °C and mean temperature above 24 °C) to identify extreme heat risk in the present and future scenario and understand what the future will look like.

The following sections outline the research framework, study area, data collection, risk calculation, and microclimate modeling processes used in this study.

2.1. Research Approach and Framework

The study follows a positivist research philosophy to achieve an empirical understanding of heat risk distribution in Lahti. A deductive approach was adopted, utilizing existing theories and frameworks on climate change, urban vulnerability, and heat risk, which were tested through spatial and statistical analyses. By leveraging multiple sources, such as climate models and demographic databases, this research enhances the evidence base for urban climate resilience planning.

2.2. Study Area

Lahti, located in Finland's Päijät-Häme region and awarded the European Green Capital in 2021, serves as the primary study area (Figure 1). Lahti's urban center, which is highly urbanized and densely populated, was chosen due to its susceptibility to urban heat risks and accessibility of relevant data. The municipality's land cover includes 74% green spaces, which influences its microclimate and urban resilience. However, the center of the city is densely built with relatively limited green infrastructure and impervious surfaces.

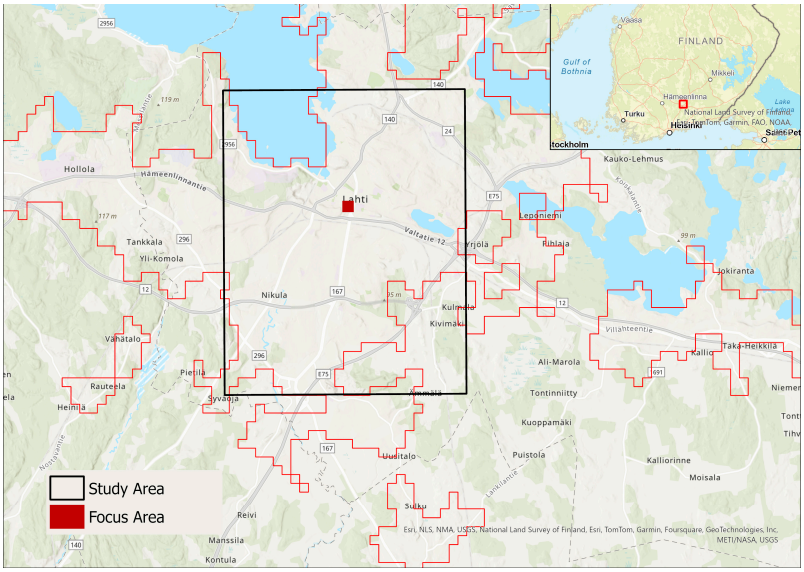


Figure 1. Location of Lahti and Study Area in the urban core.

The region of Päijät-Häme and the city of Lahti have worked towards mitigating and adapting to the risks that the changing climate will exacerbate in the future. The Climate Adaptation Plan of Päijät-Häme and the Climate change adaptation and preparedness actions in municipalities' climate plans (2023–25) are key plans that the region and the city have brought forth. The regional council has also started updating its regional risk assessments and is planning climate change preparedness tools for municipalities, communication about risks, and stormwater and heat resistance solutions [34].

2.3. Indicators for Risk Calculation

The risk assessment methodology applied Crichton's Triangle [33] to quantify risk, integrating hazard, vulnerability, and exposure indicators for each assessment unit. Key indicators included the following:

Hazard: Heat hazard was determined using LST for the present scenario and future air temperature projections. LST data were derived from Landsat satellite imagery using the maximum LST values from 2014 to 2024 in Google Earth Engine using 43 satellite images (Table 1). Future air temperatures were projected using mean monthly maximum air temperatures to capture anticipated heat risk levels under climate change scenarios.

Table 1. Dates of LANDSAT Imagery used for LST analyses.

25 July 2014	22 August 2015	5 June 2019	23 June 2020	19 June 2021	6 August 2021
25 July 2014	31 August 2016	28 June 2019	18 July 2020	3 July 2021	13 August 2021
3 August 2014	31 August 2016	30 June 2019	18 July 2020	5 July 2021	13 August 2021
3 July 2015	15 June 2017	17 August 2019	17 August 2020	5 July 2021	6 June 2022
21 July 2015	15 June 2017	7 June 2020	19 August 2020	12 July 2021	6 June 2022
20 August 2015	20 July 2018	14 June 2020	10 June 2021	12 July 2021	16 August 2022
22 August 2015	27 July 2018	23 June 2020	10 June 2021	6 August 2021	16 August 2022
12 August 2023					

Vulnerability: Vulnerability assessments considered demographic indicators such as population over 65, population under 5, population density, and employment levels. These were normalized using min-max scaling to create standardized vulnerability scores for each grid.

Exposure: Exposure metrics included built-up area percentage, impervious surface, solar exposure, proximity to water, green space cover using NDVI derived from Sentinel 2 imagery, and sky view factor (SVF). Each metric was normalized using min-max scaling to create standardized exposure scores for each grid.

The detailed methodology for quantifying the indicators is provided in Table 3. Analytical Hierarchy Process (AHP), as outlined in Section 2.5, has been used to integrate the hazard, vulnerability, and exposure profiles using spatial overlay analysis in GIS as outlined in Section 2.6.

2.4. Data Sources and Processing

Specific data for hazard, vulnerability, and exposure indicators were obtained with varying spatial resolutions, summarized in Table 2. To standardize data across resolutions, frequency-based weighting was applied to indicators within assessment units of 250 m × 250 m, as provided by the Finnish Environmental Institute. Details of the processing methodology are provided in Table 3.

Table 2. Spatial resolutions of different datasets.

Sr No.	Theme	Indicator	Source	Format	Resolution
1.	Hazard	LST	Landsat Satellite Imagery	Raster	30 m
		Future Climate Projections	EC-Earth3-veg downscaled with WorldClim v2.1 as baseline climate (EC-Earth Consortium (EC-Earth) (2019). EC-Earth-Consortium EC-Earth3-Veg model output prepared for CMIP6 CMIP. Earth System Grid Federation. DOI: https://doi.org/10.22033/ESGF/CMIP6.642, accessed on 12 November 2024)	Raster	~668 m
2.	Vulnerability	Population > 65 yrs + People requiring home care/elderly care centers	City of Lahti	Vector	250 m
		Population < 5 yrs	City of Lahti	Vector	250 m 10 m
		Weak economic status/Unemployment	City of Lahti	Vector	
		Population density	City of Lahti	Vector	
3.	Exposure	% impervious Surface	Copernicus Land Monitoring Service (Imperviousness Density 2018 (raster 10 m)—https://doi.org/10.2909/3bf542bd-eebd-4d73-b53c-a0243f2ed862, , accessed on 15 November 2024)	Raster	
		Built-up area	Copernicus Land Monitoring Service (Impervious Built-up 2018 (raster 10 m)—https://doi.org/10.2909/3e412def-a4e6-4413-98bb-42b571afd15e, accessed on 4 October 2024)	Raster	10 m
		Solar exposure	Derived using ArcGIS Pro	Raster	2 m
		Sky view factor	Derived using QGIS	Raster	2 m
		Proximity to water sources	Derived using ArcGIS Pro	Raster	30 m
		Green Areas	Derived from Sentinel 2 imagery	Raster	10 m

Table 3. Processing methodology for indicators.

	Indicator	Methodology
Hazard	Land Surface Temperature	Max LST values from 2014 to 2024 for June, July, and August (summer months) were calculated using Google Earth Engine. The maxValue raster was classified into five classes (1 to 5) and the frequency of occurrence of each class in each assessment unit was calculated in ArcGIS Pro. Each class was assigned the weights and an overall weight for each assessment unit was calculated by adding individual class values. The calculated weights were normalized by using the min-max normalization to arrive at a final Hazard value for each assessment unit.
	Air temperatures (Future)	The maximum projected future air temperatures were obtained and used to arrive at a final Future Hazard score for each assessment unit.

Table 3. *Cont.*

	Indicator	Methodology
Vulnerability	Population percentage > 65 yrs old	The percentage of the population above 65 yrs is calculated for each assessment unit. These percentages were normalized using the min-max normalization to give a final weight for this indicator per assessment unit.
	Population percentage < 5 yrs	Similar to the population percentage > 65 yrs old, the weightage of the population percentage < 5 yrs old was calculated for each assessment unit.
	Population density	Population density was calculated from the demographic data for each assessment unit. Min-max normalization was applied to translate the density on a 0 to 1 scale to ensure consistency between the different indicators.
	Employment percentage	The employment percentage was calculated by using employment data per assessment unit.
	Built-up Index	The built-up index was developed by calculating the percentage of built-up area in each assessment unit. The percentage values were normalized to translate them to a 0 to 1 scale to ensure consistency.
Exposure	Imperviousness	Imperviousness was classified into five equal classes:—0% to 20%, 20% to 40%, 40% to 60%, 60% to 80%, and 80% to 100% impervious surfaces. The frequency of occurrence of each class in each assessment unit was calculated in ArcGIS Pro. Each class was assigned weights and an overall weight for each assessment unit was calculated by adding individual class values. The calculated weights were normalized by using the min-max normalization to arrive at a final Imperviousness index for each assessment unit.
	Solar Exposure	Solar exposure was calculated at a resolution of 2 m and classified into five classes. The frequency of occurrence was calculated for each class in each assessment unit and weighted according to the weights table to arrive at a final score for the indicator for each assessment unit.
	Sky View Factor	The Sky view factor was calculated using the digital surface model at a resolution of 2 m. The frequency of occurrence was calculated for each assessment unit, weighted, and a final SVF score was calculated.
	Distance from water bodies	Distance calculated were classified into five classes and each class was assigned weights to arrive at a final weightage for each assessment unit.
	Green Areas	A similar approach was used to classify the green areas and calculate the percentage of green areas in each assessment unit. The percentage was then normalized on a 0 to 1 scale to arrive at a final weight from green areas in each assessment unit.

2.5. Analytical Hierarchy Process (AHP)

To weight indicators in risk calculation, the Analytical Hierarchy Process (AHP) was employed. This process involved pairwise comparisons between indicators based on expert input from Lahti city's urban designer and the general plan architect. Weightage for each indicator was calculated to reflect the relative importance of factors influencing heat risk in the area, with higher weights indicating greater influence on overall risk. Table 4 shows the final AHP weights for each of the indicators in the study.

Table 4. AHP weights for each of the indicators.

Sr No.	Theme	Indicator	Weight
2.	Vulnerability	Population > 65 yrs + People requiring home care/elderly care centers	0.5
		Population < 5 yrs	0.2
		Weak economic status/Unemployment	0.1
		Population density	0.2
3.	Exposure	% impervious Surface	0.17
		Built-up area	0.17
		Solar exposure	0.17
		Sky view factor	0.31
		Proximity to water sources	0.11
		Green Areas	0.07

2.6. GIS and Overlay Analysis

The risk calculation utilized ArcGIS Pro to map and analyze heat risk distribution. Spatial overlays combined hazard, vulnerability, and exposure layers using weightage derived using AHP to generate a composite heat risk map for Lahti. These maps identified

high-risk zones and provided a foundation for evaluating the mitigative capacity of existing urban plans.

2.7. Microclimate Modeling with ENVI-Met

ENVI-met version 5.6.1 software was used to model microclimate conditions and evaluate thermal comfort in high-risk areas. ENVI-met is a holistic 3-D non-hydrostatic model for the simulation of surface-plant-air interactions most often used to simulate urban environments and to assess the effects of green architecture visions. It operates at a microscale (0.5–10 m resolution, 24–48 h timeframe). The model outputs include short wave and long wave radiation fluxes, plant transpiration/evaporation and sensible heat flux, dynamic surface/wall temperatures, soil water/heat exchange inside soil systems, and 3-D vegetation water balance. It also models gas/particle dispersion and biometeorological indices like MRT, PMV/PPD, PET, and UTCI using the BioMet module [35]. Two modeling scenarios were developed to assess thermal comfort during a very hot day condition defined by the Finnish Meteorological Institute as a day where the maximum daily temperature is above 30 °C and the mean temperature is above 24 °C as follows:

Scenario 1: Modeled for a maximum air temperature of 30.4 °C, representing a hot day in June 2024. The simulation ran for 24 h, allowing for a detailed analysis of diurnal temperature variation.

Scenario 2: Projected for 2040, this scenario used future maximum monthly temperature data (see Table 2 for data source) for June 2040 to estimate conditions during a similar summer day.

For each scenario, ENVI-met simulated urban morphology with specific details on building height, materials, vegetation, and surface types. The parameterization of the model has been detailed in Table 5. The model's accuracy was validated against real data from a weather logger station in Lahti as detailed in Section 3.6.

Table 5. Parameters used for ENVI-Met Modeling.

Parameter	Description	Value	
Computational domain and grid	Model Dimension	129 × 129 × 25	
	Grid Cells (*dx*,*dy*,*dz*)	3 × 3 × 5	
	Nesting grids	5	
		dz of lowest grid box is split into five cells	
	Telescoping	20% after 100 m	
Surfaces and Materials	Building walls	Passive wall good insulation	
	Building roofs	Passive wall good insulation	
	Soil type	Default Unsealed Soil (Sandy Loam)	
	Other areas	Asphalt	
Vegetation	Trees	*Tilia*	
	Grass	Grass cover (25 cm average dense)	
General Settings		**Scenario 1**	**Scenario 2**
	Maximum Air temperature	30	33
	Minimum Air Temperature	16	18
	Time of Max. Air Temperature	18:00	18:00
	Time of Min. Air Temperature	05:00	05:00
	Maximum Relative Humidity	81	81
	Minimum Relative Humidity	29	29
	Time of Min. Rel. Humidity	20:00	20:00
	Time of Max. Rel. Humidity	05:00	05:00
Bio-Met (UTCI)	Age (y); Weight (kg); Height; Gender	65, 70 kg, 1.8 m, Male	
	Body Position	Standing	
	Walking speed (m/s)	1.21 m/s	
	Clothing parameters (clo.)	0.5 clo	

2.8. Universal Thermal Climate Index (UTCI)

To evaluate outdoor thermal comfort, the Universal Thermal Climate Index (UTCI) was applied, providing a standardized measure that integrates air temperature, wind speed, humidity, and radiant temperature. The Universal Thermal Climate Index (UTCI) has been used for assessing outdoor thermal climate. It incorporates factors such as air temperature,

wind speed, humidity, and radiant temperature to provide a comprehensive measure of thermal stress experienced by individuals. As a standardized metric, UTCI enables comparisons across various climates and regions, supporting public health recommendations, infrastructure planning, and climate adaptation efforts [36–38]. Figure 2 shows the inputs to UTCI and the equivalent temperature.

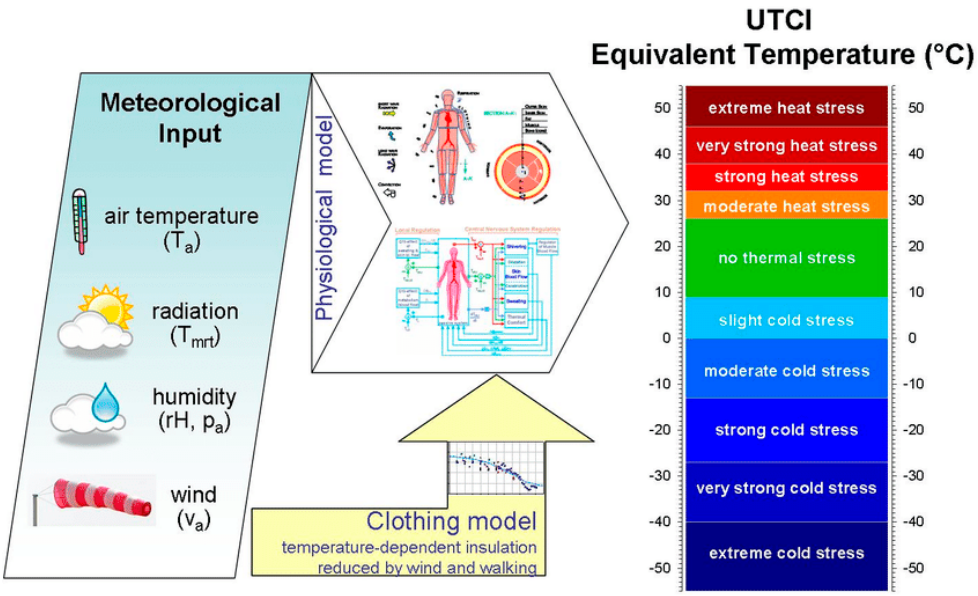


Figure 2. UTCI model and equivalent temperature scale [39].

3. Results

3.1. Climate Change and Temperature Trends in Lahti

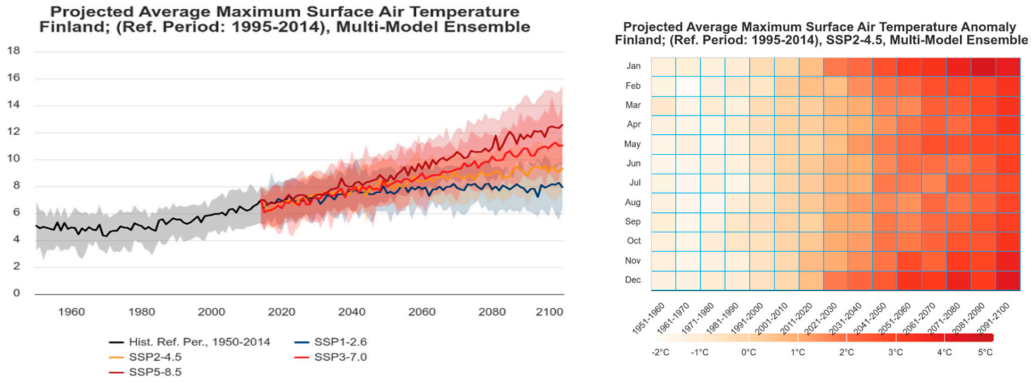
The city of Lahti is already witnessing substantial increases in air temperature, reflective of larger climate trends observed across Finland. According to the World Bank's Climate Change Knowledge Portal, Finland's climate has shown a steady warming trend, which is corroborated by Finnish Meteorological Institute (FMI) data on temperature anomalies. Lahti, in particular, recorded summer temperature anomalies reaching up to 2.7 °C above the 1991–2020 baseline, with extreme anomalies observed in June, peaking at 5 °C in 2021. Figure 3 demonstrates the temperature anomalies and the increasing trend, emphasizing that Lahti is experiencing more frequent and severe temperature extremes.

3.2. Land Surface Temperature (LST) Analysis and Hazard Mapping

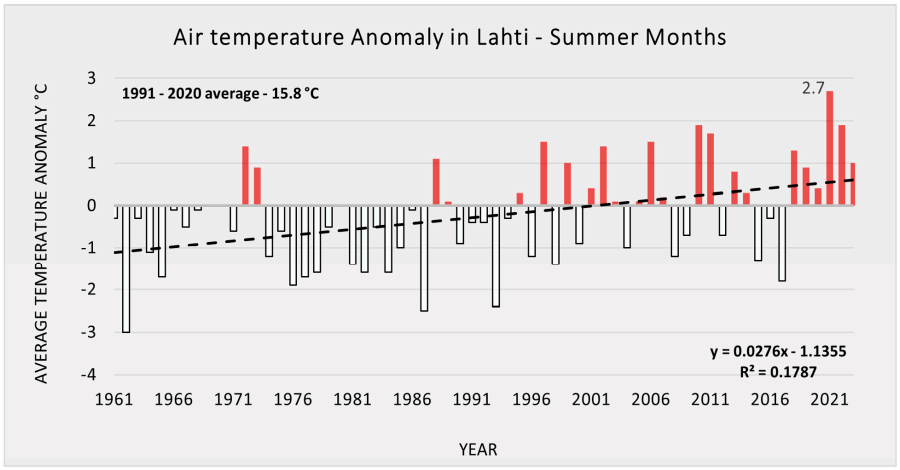
Satellite-based analysis of Land Surface Temperature (LST) highlights considerable variability across Lahti's land cover types. Data collected from 2014 to 2024 reveal that LST can vary up to 22 °C across land use and land cover (LULC) types in Lahti, with the urban core showing significantly higher temperatures than surrounding green or water-covered areas. Figure 4 presents LST profiles for Lahti, illustrating the concentration of higher temperatures in built-up zones, while water bodies consistently maintain lower LST values.

During a recent heatwave on June 27, 2024, this pattern was even more pronounced, with LST differences reaching 24 °C between urban and natural areas. This LST analysis underscores the importance of addressing land use changes as a key factor in mitigating future heat hazards.

a) Future Projections of Climate change in Finland (Source: World Bank Climate change knowledge portal)



b) Air temperature anomalies in Lahti in the summer months (Source: FMI)



c) Mean monthly air temperature trend, Vesijärvenkatu, Lahti

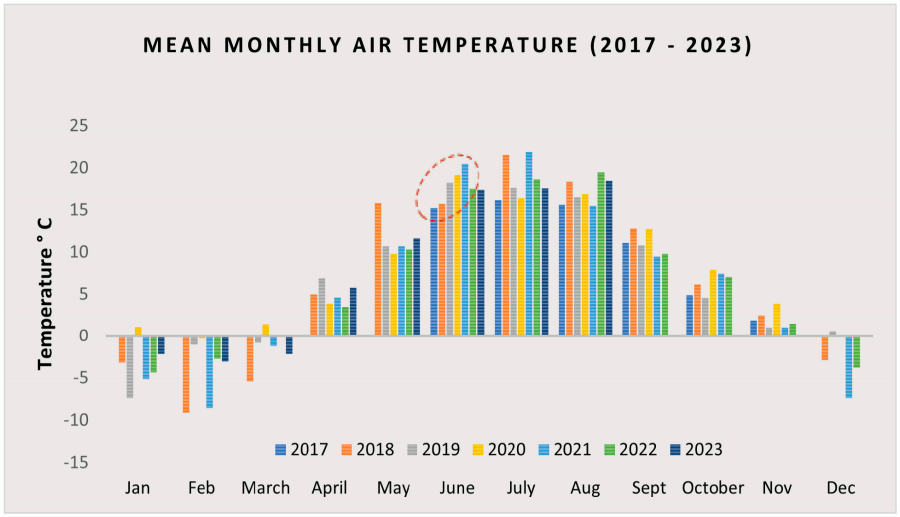


Figure 3. Changing temperatures in Finland and Lahti (Data Source (**c**): Turku Urban Climate Research Group (TURCLIM), Geography Division, University of Turku, Finland).

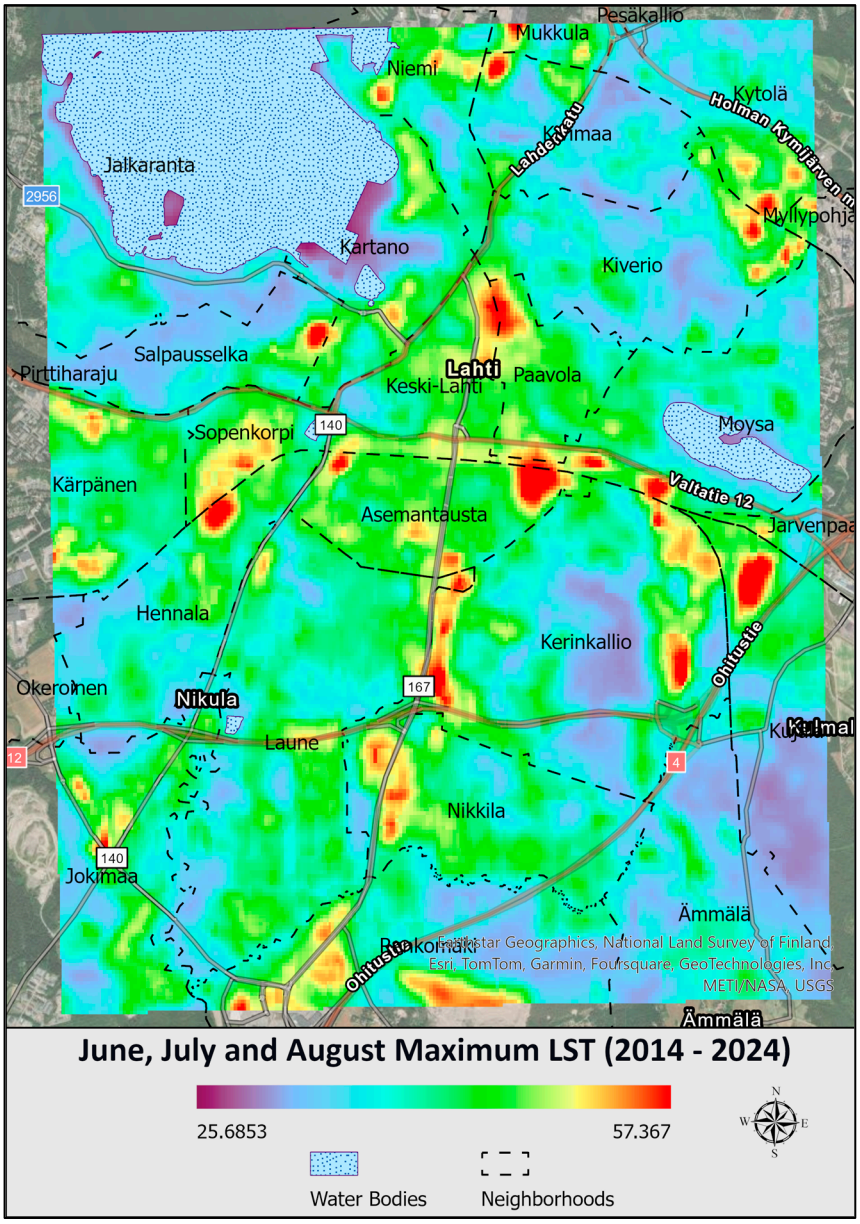


Figure 4. Land Surface Temperature profile of the Study area.

3.3. Vulnerability Assessment

The vulnerability analysis of Lahti's population reveals demographic shifts that will likely intensify future heat-related risks. The elderly population, particularly those over 65, is projected to increase by 13.2% by 2040, while populations under 5 years old are expected to decrease. Vulnerability mapping across Lahti indicates minor changes overall, with the exception of a noticeable increase in areas categorized as "Very High" vulnerability, where elderly populations are most concentrated, showing a 55% increase in areas with "Very High" vulnerability. This demographic shift is critical, as it highlights the need for mitigation geared towards supporting older adults during extreme heat events. The analysis also supports input from Lahti city officials, who prioritized older adults as a critical factor in vulnerability assessments using the Analytical Hierarchy Process (AHP).

3.4. Exposure Assessment

Urbanization and changes in land use contribute significantly to the exposure index for heat risk in Lahti. This study assessed six exposure indicators. Of these, the built-up area

showed the most notable change, with a projected 147% increase in the highest exposure category (Class 5) by 2040.

Although green spaces have a relatively stable presence, they show minor increases in higher exposure zones. This increase is a positive aspect of Lahti's 2035 masterplan, as green areas can mitigate urban heat risk. However, the increase in green areas may not mitigate the rapid expansion of built-up surfaces, suggesting a need for further green infrastructure initiatives integrated into urban development.

3.5. Heat Risk Profile

Integrating hazard, vulnerability, and exposure, the risk profile of Lahti projects substantial growth in high-risk zones by 2040. Figure 5a,b show the current and future heat risk maps, with significant increases observed in the "High" and "Very High" risk categories.

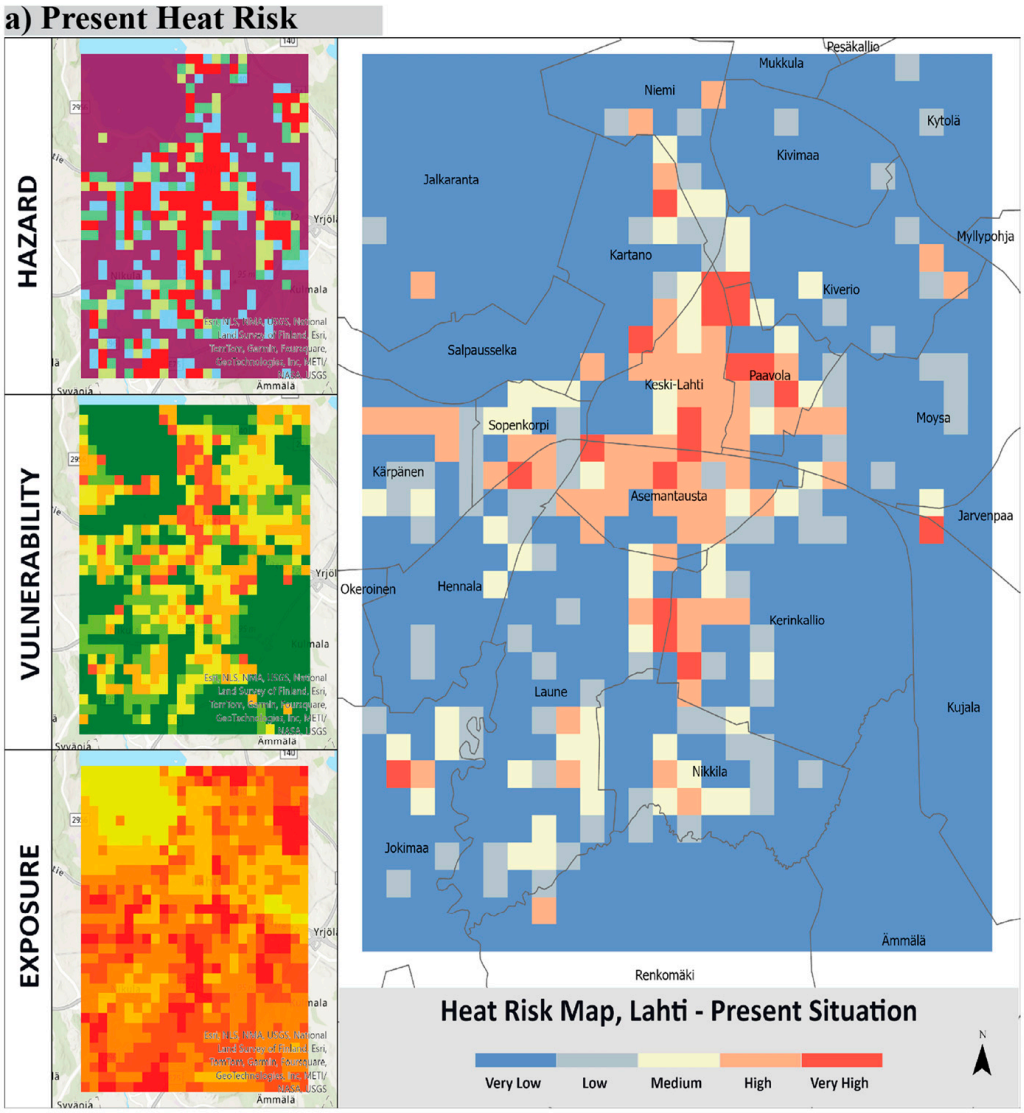


Figure 5. *Cont.*

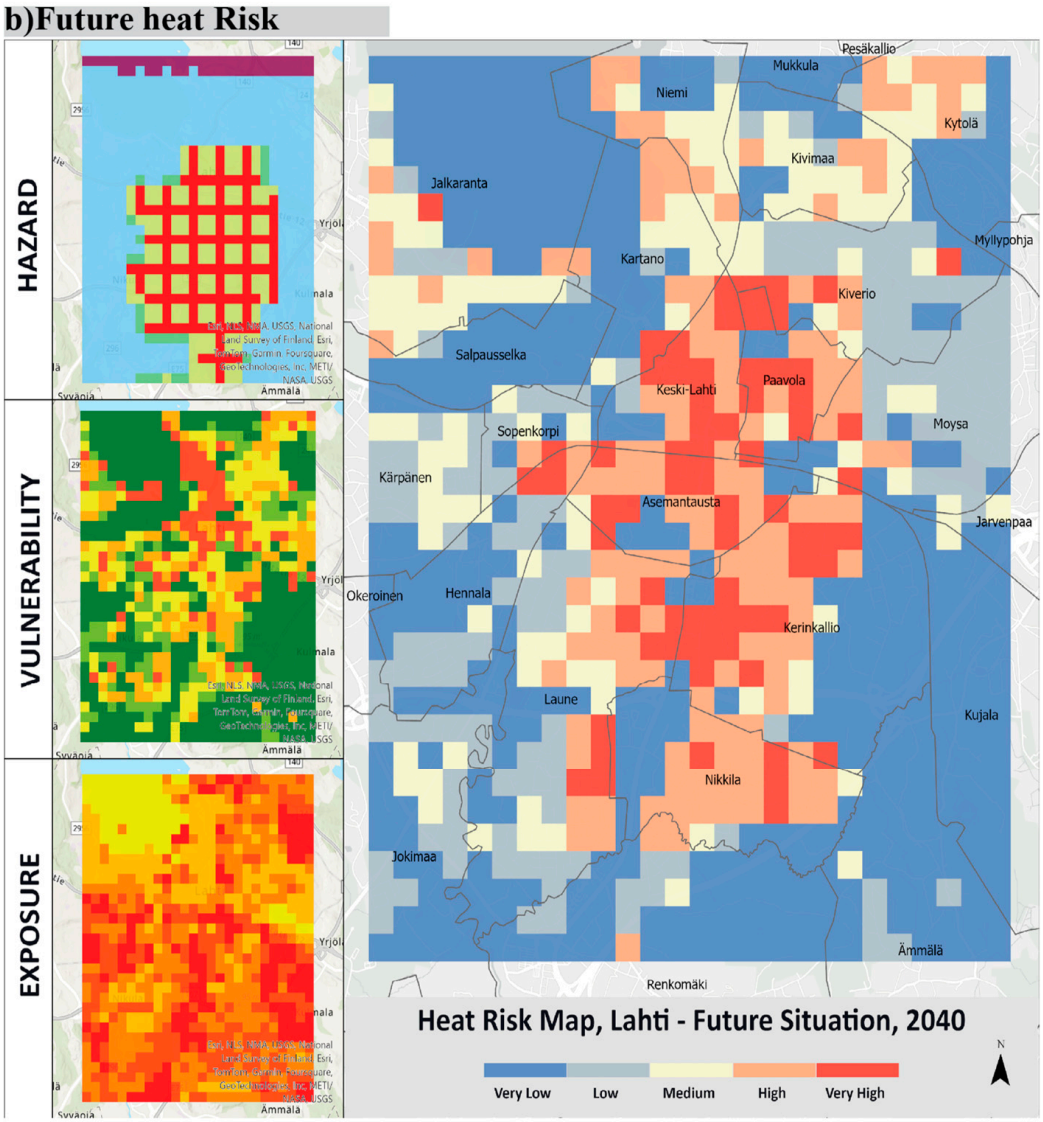


Figure 5. (**a**) Present Risk Profile of the Study Area; (**b**) Future Heat Risk Profile of the Study Area.

The increase in high-risk zones underscores the combined effect of rising temperatures, increased urban density, and an aging population, all contributing to Lahti's elevated susceptibility to extreme heat. These findings highlight the need for targeted interventions in high-risk areas to protect vulnerable populations and infrastructure from anticipated climate impacts.

3.6. Microclimate Simulation: Present and Future Conditions

ENVI-met modeling was conducted for a high-risk residential assessment unit, considering present and future conditions. Calibration runs demonstrated good model accuracy with respect to the nearby Vesijärvenkatu weather data logger, with a Root Mean Square Error (RMSE) of 1.1 °C.

In Scenario 1, a hot day in June 2024 was simulated, highlighting that asphalt surfaces reached a maximum temperature of 28.8 °C, while Scenario 2, simulating a similar day in 2040, showed increased surface temperatures of up to 5.9 °C in asphalt-covered areas.

The Universal Thermal Climate Index (UTCI) for the future scenario indicates increased thermal stress, with UTCI values reaching up to 42.75 °C, marking a 3.7 °C rise compared to the present day (Figure 6). These projections underscore the need for adaptive infrastructure to reduce urban heat stress in the future.

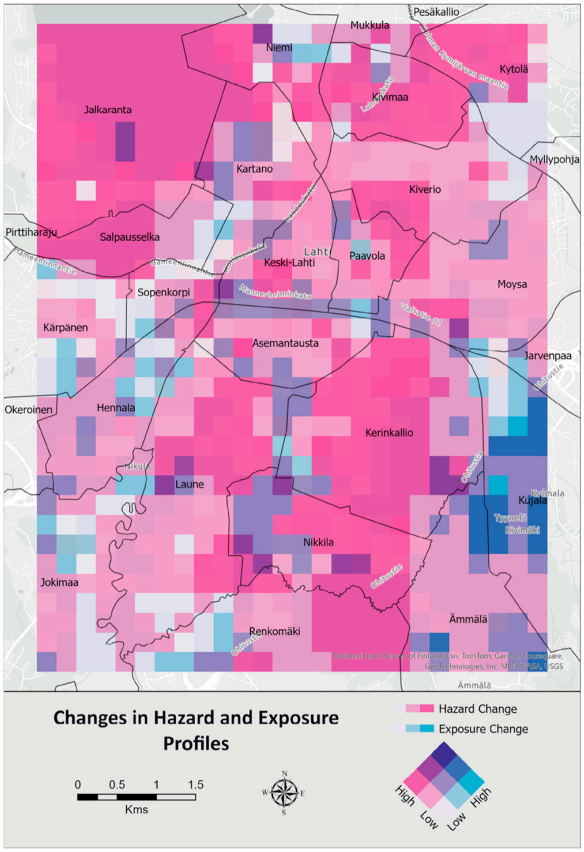


Figure 6. Bivariate Analysis for Hazard and Exposure.

4. Discussion

4.1. Mapping Heat Hazards, Vulnerabilities, and Exposure

The assessment of heat hazards, vulnerabilities, and exposure in Lahti highlights significant urban and demographic factors influencing heat risk. The choice of indicator variables—such as temperature, age demographics, and urban cover—provides a comprehensive profile of risk factors in Lahti. However, the outcomes underscore the challenges of using multi-criteria decision-making methods when dealing with spatial data of varying resolutions, ranging from 2 m to 250 m grids. This variability can impact the generalizability and precision of results.

The spatial analysis reveals that high-risk areas in Lahti are concentrated in urbanized zones with minimal vegetation and a high density of built structures. This finding aligns with previous studies [40,41], which report that urbanization intensifies land surface temperatures (LST) due to increased impervious surfaces. In Lahti, the emphasis on demographic vulnerability—particularly the growing elderly population—further supports the risk profile by revealing a concentration of vulnerable individuals in urban centers. Since population and urban structures are dynamic in nature, regular updates to these risk assessments are essential for adapting to demographic shifts and changing urban landscapes.

Using bivariate analysis, it can be concluded that the primary reason for the change in risk profile is the changing hazard profile. Hazard input in risk has a big impact as seen from the hazard change-vulnerability change and hazard change-exposure change bivariate analysis (Figures 6–8). This is an expected outcome as vulnerability and exposure in the future scenario do not estimate large changes.

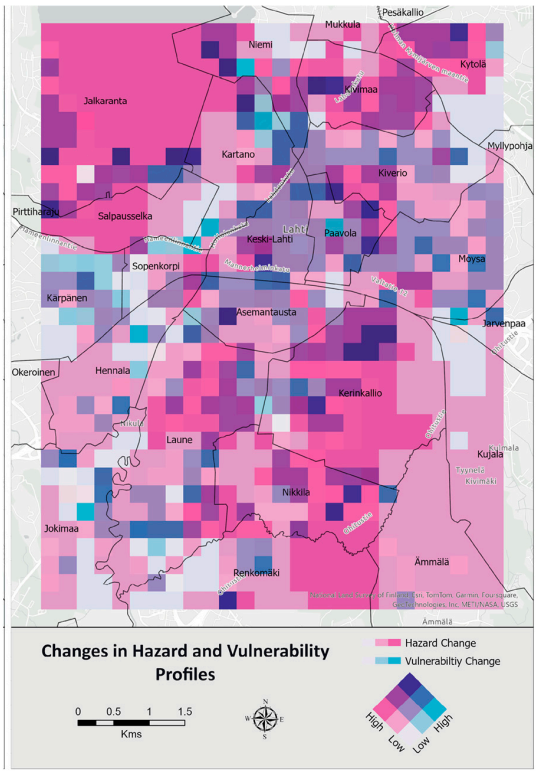


Figure 7. Bivariate Analysis for Hazard and Vulnerability.

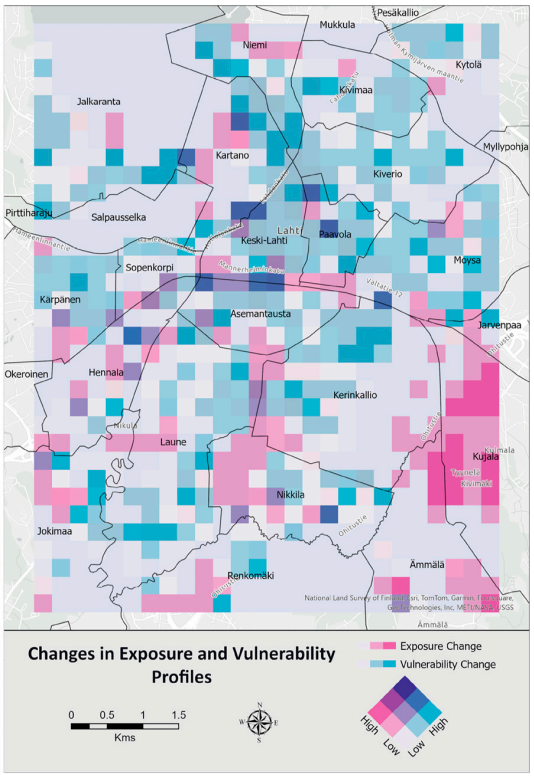


Figure 8. Bivariate Analysis for Vulnerability and Exposure.

4.2. Microclimate Modeling and Mitigation Strategies

ENVI-met modeling provides insights into microclimatic conditions in Lahti, showing that urbanized, concretized areas without vegetation are prone to high Mean Radiant Temperatures (MRT), amplifying thermal discomfort beyond air temperature alone. The MRT analyses suggest that even modest vegetation, as seen in sample point B in Figure 9

with street vegetation, significantly reduces MRT compared to point A, which is devoid of greenery. Studies by [42,43] highlight similar patterns in other urban environments, confirming these findings.

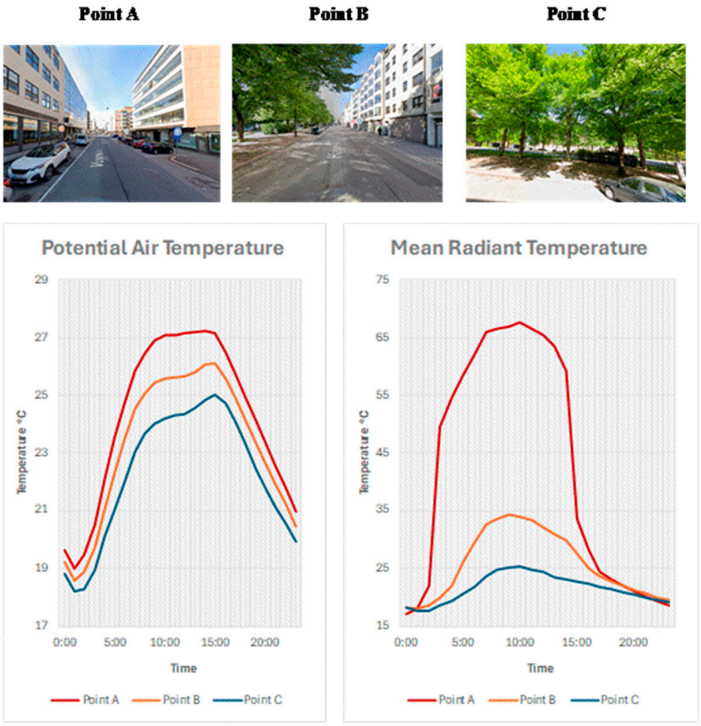


Figure 9. Potential air temperature and Mean Radiant temperature for sample points.

The Universal Thermal Climate Index (UTCI) analysis underscores the need for adaptive strategies, showing that current urban areas will likely experience more frequent periods of "strong" or "very strong" heat stress as temperatures rise. Points with greenery, such as point C in Figure 10, consistently exhibit lower UTCI values, suggesting that green spaces contribute significantly to lowering heat stress levels. Based on these findings, Lahti's urban planning could benefit from integrating shading and vegetation as practical measures to reduce thermal stress, especially in heavily urbanized zones. Future studies could expand on this by examining the cooling effects of different vegetation types or relationships to optimize cooling in Lahti's specific climate. Table 6 shows the UTCI comfort hours for present and future scenarios highlighting the impact of vegetation.

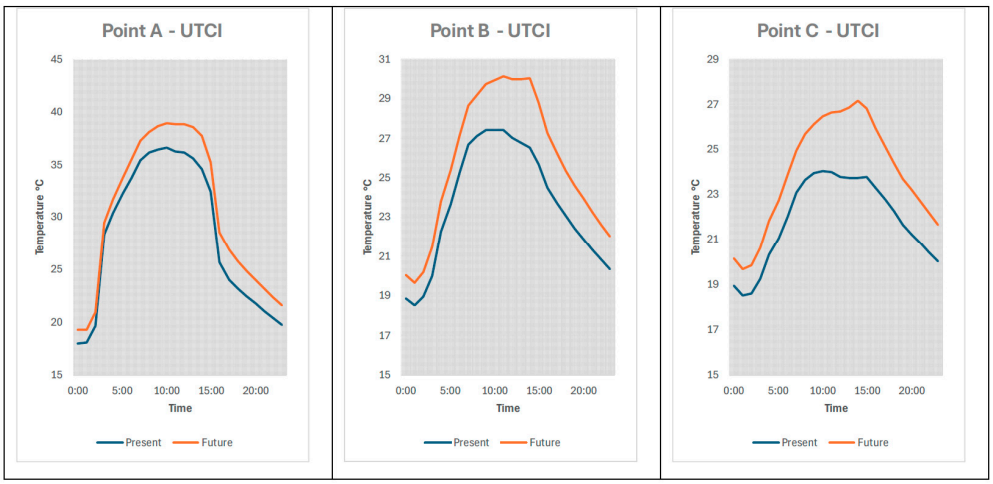


Figure 10. UTCI comparison for sample points for Present and Future Scenarios.

Table 6. UTCI Thermal perception hours.

UTCI Thermal Perception	No. of Hours in a Day					
	Point A		Point B		Point C	
	Present	Future	Present	Future	Present	Future
No Thermal Stress	11	9	16	12	0	17
Moderate Heat Stress	2	4	8	12	0	7
Strong Heat Stress	11	5	0	0	0	0
Very Strong Heat stress	0	6	0	0	0	0

4.3. Assessing the Effectiveness of High-Albedo Surfaces

A test case utilizing high-albedo materials on streets showed mixed results; while these surfaces reduce ambient air temperatures, they increase MRT and UTCI values, potentially worsening discomfort at street level as seen in Figure 11. This finding aligns with [44] work, which reported higher reflectivity causing thermal discomfort in courtyards, and [45], who suggested that albedo changes have a limited impact on UTCI. These findings imply that high-albedo materials may not be suitable for densely populated pedestrian areas in Lahti, where increased reflectivity could exacerbate heat stress for individuals at ground level. An alternative approach could focus on integrating shading solutions in areas where MRT is likely to be high. Future research could examine the combined effect of shading and high-albedo materials to balance the cooling effects of both strategies while minimizing their drawbacks.

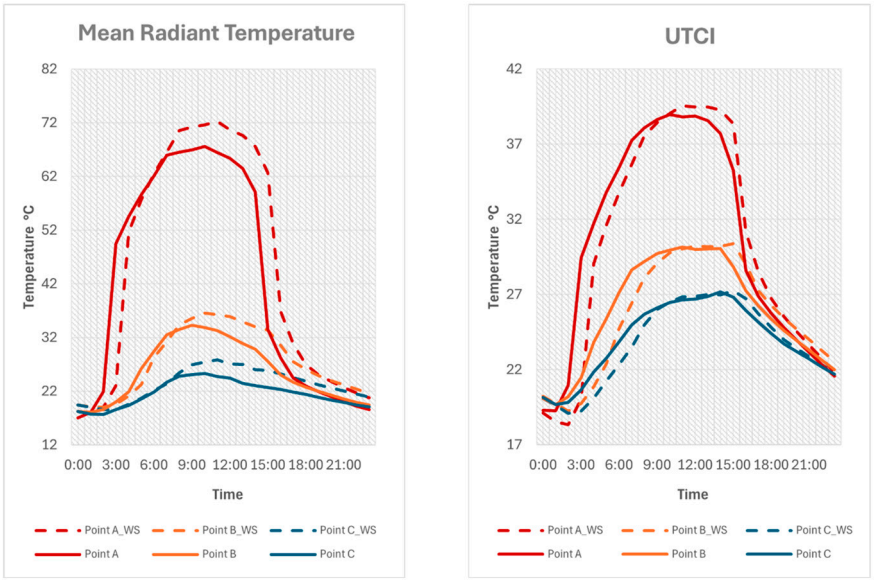


Figure 11. MRT and UTCI for high-albedo street simulation.

4.4. Correlation Analysis of Vulnerability, Exposure, and Hazard Indices with Future Risk

The correlation analysis between the modeled risk and the indices used in the Analytical Hierarchy Process (AHP) provides insights into the reliability of the methodology. The Vulnerability Index (VI) exhibited a strong positive correlation ($r \approx 0.838$) with the modeled risk, highlighting its significance as a key determinant. The Exposure Index (EI) showed a weaker correlation ($r \approx -0.162$). This weaker correlation is likely attributable to the low variance (0.00859) observed in EI relative to VI, which may reduce its statistical association with the modeled risk highlighting the importance of the development of risk indices to highlight at-risk areas.

Further analysis of individual vulnerability indicators revealed positive correlations with risk, including population density ($r \approx 0.590$), population over 65 years ($r \approx 0.505$), unemployment ($r \approx 0.360$), and population under 6 years ($r \approx 0.199$), underpinning the role of socio-economic factors in influencing risk. Similarly, correlations for exposure indicators showed moderate associations, with built-up areas ($r \approx 0.502$) and impervious surfaces ($r \approx 0.499$) being the most correlated factors indicating that urbanization and surface sealing contribute extensively to modeled risk. The hazard index (HI) derived from LST showed a strong positive correlation to the modeled future risk ($r \approx 0.764$).

Scatterplots (Figures 12–14) further illustrate these relationships, providing evidence of trends between the indices and the modeled risk. These scatterplots highlight the relationship between VI and risk, as well as the weaker association for EI, supporting the observation of low variance in EI. The scatterplot for HI demonstrates a clear positive trend, reinforcing the influence of hazard factors on future risk projections.

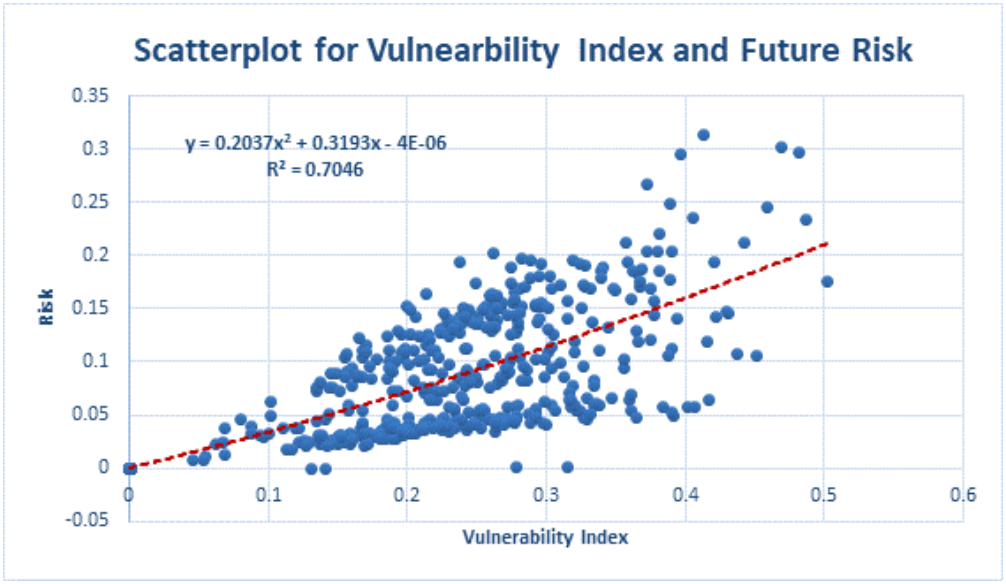


Figure 12. Scatterplot for Vulnerability index and modeled future risk.

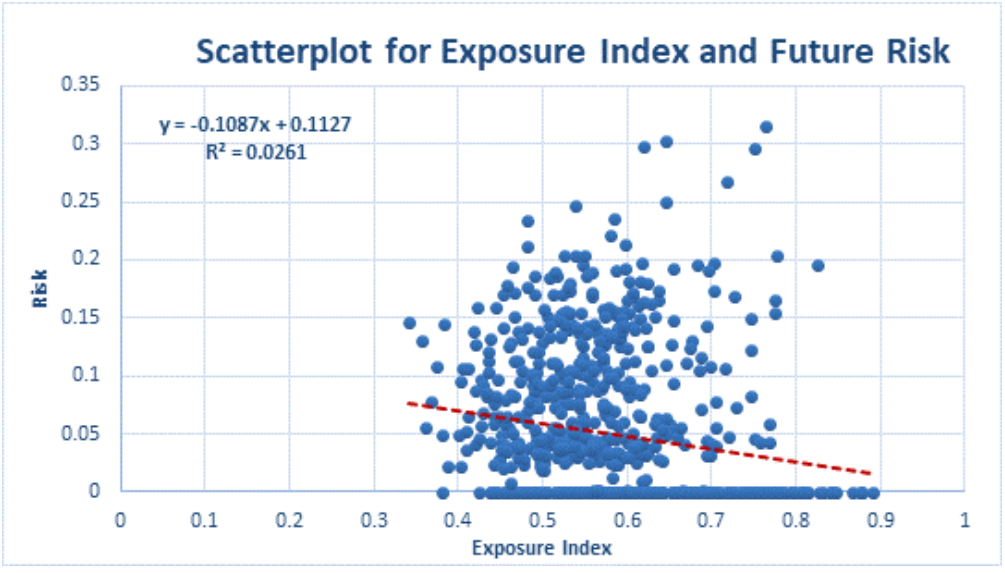


Figure 13. Scatterplot for Exposure index and modeled future risk.

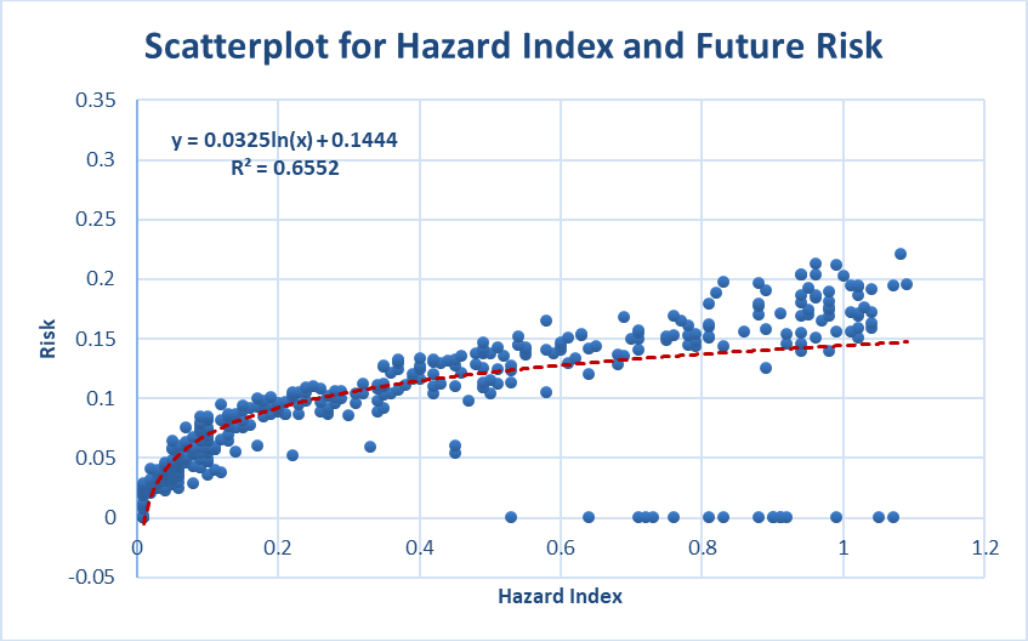


Figure 14. Scatterplot for Hazard index and modeled future risk.

4.5. Risk Profile Implications and Urban Planning

The projected rise in mean summer temperatures by 2040 will substantially increase the number of high-risk zones in Lahti, especially as the city experiences rapid urbanization. Correlation analyses demonstrate that the spatial distribution of vulnerability factors influences the intensity and location of heat risk zones greatly, with the concentration in the city center leading to more high-risk zones as compared to suburban areas.

Given these findings, Lahti's future urban plans must consider the growing vulnerability of its elderly population and the concentration of this section of society in the highly exposed areas in the city center. This means adaptation measures to target heat risk should be prioritized in these high-risk zones. City center area tends to have limited space and more impervious surfaces, therefore adaptation measures such as decentralizing elderly services to lower-risk areas, integration of green infrastructure, temporary shading structures, and usage of high albedo surfaces can be explored.

One of the measures simulated in this study is the application of high-albedo surfaces as an intervention to mitigate heat risk. However, as highlighted in Section 4.3, prioritizing the development of green infrastructure in high-density built-up areas should be considered as a more effective alternative to high-albedo surfaces. The use of high-albedo surfaces can be piloted for building rooftops; however, additional studies are recommended to fully comprehend the impact of this on the microclimatic condition in Lahti.

Alternatively, seasonal shading structures, including pergolas, retractable coverings, and summer huts, are recommended to reduce heat exposure and enhance urban thermal comfort. Their temporary nature allows for easy removal during winter, ensuring adaptability to changing weather conditions.

These findings also indicate a need for sensitivity analysis in urban planning, as the dynamic nature of demography in Lahti could alter risk profiles rapidly. Given the complex interactions between urban form, demographics, and climate variables, a sensitivity analysis is essential to ensure adaptation measures are tailored to specific contexts and risk profiles.

5. Conclusions

Lahti faces increasing heat risk due to rising summer temperatures, necessitating targeted urban planning measures that combine actions in the short term with long-term solutions. In the short term, urban infrastructure design adjustments are crucial. With high seasonal variation in urban temperatures, exploring multifunctional cooling strategies beyond vegetation—such as innovative building materials, urban water features, and temporary shading structures—will be essential to enhance thermal comfort in Lahti while also providing other utilities in colder weather.

As seen from Table 6, Point C, a green location, would be under moderate heat risk for ~30% of the day while urban, concretized areas such as sample Point A will remain under strong heat stress for 20% of the day and very strong heat stress for 25% of the day. Thus, for long-term resilience, enhancing Lahti's green and blue infrastructure will play a pivotal role. While Lahti and Finland in general have extensive green areas and forests, integrating more green areas in the high heat-risk hotspots in urban areas is the need of the hour. As the European Green Capital, Lahti already benefits from extensive forests around the city that can be further integrated into urban planning and zoning regulations for new development. Drawing inspiration from Helsinki, Lahti can implement green roofs tailored to its needs to mitigate and adapt to rising temperatures. Adapting tools such as the green factor method of the city of Helsinki to the local context can provide insights to assist planning for green infrastructure. Microclimate modeling using ENVI-met further highlights the cooling potential of green areas in a densely urban environment in Lahti. Additionally, Lahti's abundant water bodies offer opportunities to develop and integrate a blue infrastructure network to combat heat risks. Developing water catchment areas in urban developments can provide localized cooling as well as mitigate flooding risks, improve water quality, and contribute to climate adaptation.

Microclimate analysis using ENVI-met offers valuable insights into thermal comfort. This study acts as a pilot for city planners to model interventions and their impacts, enabling data-driven decisions to optimize urban designs for reduced surface and air temperatures. Furthermore, the study identifies the need to establish a denser network of weather data loggers that will further enhance planning by offering high-resolution, continuous data. This network will allow for more localized heat risk assessments, monitoring the effectiveness of implemented measures over longer periods, guiding adaptive strategies to the changing climate, and providing data for periodic updates to risk assessments, as demographic and climate patterns evolve. Regular assessments would ensure that Lahti's urban resilience strategies remain effective and responsive to emerging challenges, providing a model that other Finnish cities could follow to address similar heat-related risks.

Although the study focuses on the city of Lahti, the methodology utilized is scalable and replicable and hence can be used as a building block for heat risk assessments in other cities in Finland. This study further provides a foundation for future research in several areas. Firstly, studies examining household-level data could provide finer insights into vulnerability factors, particularly in high-risk urban areas. With well-insulated buildings unsuited for rising temperatures, future research can investigate the combined thermal comfort of indoor and outdoor spaces. Furthermore, it is imperative that the City of Lahti explores optimal configurations of green infrastructure, focusing on specific types of vegetation or layouts to maximize cooling effects within limited urban space.

Lahti's approach to urban adaptation is underpinned by policies and plans at local, regional, and national levels. The Päijät-Häme Climate Adaptation Plan (2023–2030) and Lahti's Masterplan 2035 serve as key instruments for embedding climate resilience into urban development. Finland's National Climate Change Adaptation Plan 2022 provides strategic guidance for integrating adaptation measures across multiple governance levels,

ensuring cohesive and long-term resilience. Through the implementation of suggested measures in accordance with these strategies, Lahti is well-positioned to mitigate future heat risks, enhance urban thermal comfort, and strengthen its capacity to address the impacts of the changing climate.

Author Contributions: Conceptualization, A.N., R.E. and E.A.; methodology, A.N., R.E. and E.A.; software, R.E.; validation, A.N.; formal analysis, A.N.; investigation, A.N.; resources, R.E. and E.A.; data curation, A.N.; writing—original draft preparation, A.N.; writing—review and editing, R.E. and E.A.; visualization, A.N.; supervision, R.E. and E.A.; project administration, R.E.; funding acquisition, R.E. and E.A. All authors have read and agreed to the published version of the manuscript.

Funding: This research was funded by the European Commission—European Education and Culture Executive Agency (EACEA), grant number 619644.

Institutional Review Board Statement: Not applicable.

Informed Consent Statement: Not applicable.

Data Availability Statement: Original data is unavailable due to ethical reasons.

Acknowledgments: The authors would like to acknowledge the contributions and support of Johanna Säaksniemi, Yleiskaava-arkkitehti (General Plan Architect), and Jaakko Tikkala, as well as Suunnitteluinsinööri (Planning Engineer) for support in collecting and collating demographic data pertaining to Lahti City, and Juuso Suomi, Turku Urban Climate Research Group (TURCLIM), Geography Division, University of Turku for providing air temperature data that underpins Figures 2 and 4.

Conflicts of Interest: The authors declare no conflicts of interest. The funders had no role in the design of the study; in the collection, analyses, or interpretation of data; in the writing of the manuscript; or in the decision to publish the results.

References

1. Ibebuchi, C.C.; Abu, I.O. Characterization of temperature regimes in Western Europe, as regards the summer 2022 Western European heat wave. *Clim. Dyn.* **2023**, *61*, 3707–3720. [CrossRef]
2. Hoy, A.; Hänsel, S.; Maugeri, M. An endless summer: 2018 heat episodes in Europe in the context of secular temperature variability and change. *Int. J. Climatol.* **2020**, *40*, 6315–6336. [CrossRef]
3. Woolway, R.I.; Jennings, E.; Carrea, L. Impact of the 2018 European heatwave on lake surface water temperature. *Inland Waters* **2020**, *10*, 322–332. [CrossRef]
4. Neuwirth, B.; Rabbel, I.; Bendix, J.; Bogena, H.R.; Thies, B. The european heat wave 2018: The dendroecological response of oak and spruce in western Germany. *Forests* **2021**, *12*, 283. [CrossRef]
5. Website, N.I.; Ni, C. A Milestone in UK Climate History. 2022. Available online: https://climatenorthernireland.org.uk/a-milestone-in-uk-climate-history/ (accessed on 4 December 2024).
6. Intergovernmental Panel on Climate Change (IPCC). *Climate Change 2022—Impacts, Adaptation and Vulnerability: Working Group II Contribution to the Sixth Assessment Report of the Intergovernmental Panel on Climate Change*; Cambridge University Press: Cambridge, UK, 2023. [CrossRef]
7. Coumou, D.; Robinson, A. Historic and future increase in the global land area affected by monthly heat extremes. *Environ. Res. Lett.* **2013**, *8*, 034018. [CrossRef]
8. Perkins-Kirkpatrick, S.E.; Lewis, S.C. Increasing trends in regional heatwaves. *Nat. Commun.* **2020**, *11*, 3357. [CrossRef]
9. Domeisen, D.I.; Eltahir, E.A.; Fischer, E.M.; Knutti, R.; Perkins-Kirkpatrick, S.E.; Schär, C.; Seneviratne, S.I.; Weisheimer, A.; Wernli, H. Prediction and projection of heatwaves. *Nat. Rev. Earth Environ.* **2023**, *4*, 36–50. [CrossRef]
10. Seneviratne, S.I.; Zhang, X.; Adnan, M.; Badi, W.; Dereczynski, C.; Di Luca, A.; Ghosh, S.; Iskander, I.; Kossin, J.; Lewis, S. *Weather and Climate Extreme Events in a Changing Climate*; Cambridge University Press: Cambridge, UK, 2021; Chapter 11. [CrossRef]
11. Kim, S.; Sinclair, V.A.; Räisänen, J.; Ruuhela, R. Heat waves in Finland: Present and projected summertime extreme temperatures and their associated circulation patterns. *Int. J. Climatol.* **2018**, *38*, 1393–1408. [CrossRef]
12. Ruosteenoja, K.; Jylhä, K. Average and extreme heatwaves in Europe at 0.5–2.0 C global warming levels in CMIP6 model simulations. *Clim. Dyn.* **2023**, *61*, 4259–4281. [CrossRef]
13. Finnish Meteorological Institute. New All-Time High Temperature Record in Finland: 37.2 °C Measured in Joensuu on 29 July 2010. 2010. Available online: https://en.ilmatieteenlaitos.fi (accessed on 3 October 2024).

14. Sinclair, V.A.; Mikkola, J.; Rantanen, M.; Räisänen, J. The summer 2018 heatwave in Finland. *Weather* **2019**, *74*, 403–409. [CrossRef]
15. Finnish Meteorological Institute. Climate Change in Finland: Warming Trends and Temperature Increases. 30 September 2021. Available online: https://en.ilmatieteenlaitos.fi (accessed on 8 October 2024).
16. Finnish Meteorological Society. Finnish Climate Is Expected to Change More During Winter Than During Summer Months. 2017. Available online: https://en.ilmatieteenlaitos.fi/news/400026370 (accessed on 7 November 2024).
17. City of Helsinki, Urban Environment Division. *Weather and Climate Change Risks in Helsinki* (Publications of the Urban Environment Division 32/2019). 2019. Available online: https://www.hel.fi/static/liitteet/kaupunkiymparisto/julkaisut/julkaisut/julkaisu-32-19-en.pdf (accessed on 8 October 2024).
18. Ruosteenoja, K.; Jylhä, K.; Kämäräinen, M. Climate projections for Finland under the RCP forcing scenarios. *Geophysica* **2016**, *51*, 17–50.
19. Mikkonen, S.; Laine, M.; Mäkelä, H.M.; Gregow, H.; Tuomenvirta, H.; Lahtinen, M.; Laaksonen, A. Trends in the average temperature in Finland, 1847–2013. *Stoch. Environ. Res. Risk Assess.* **2015**, *29*, 1521–1529. [CrossRef]
20. Astone, R.; Vaalavuo, M. Climate change and health: Consequences of high temperatures among vulnerable groups in Finland. *Int. J. Soc. Determ. Health Health Serv.* **2023**, *53*, 94–111. [CrossRef]
21. Government Report on Finland's National Climate Change Adaptation Plan Until 2030 Finnish Government. Finland's National Climate Change Adaptation Plan Until 2030. 2024. Available online: https://julkaisut.valtioneuvosto.fi (accessed on 10 November 2024).
22. Veijalainen, N.; Ahopelto, L.; Marttunen, M.; Jääskeläinen, J.; Britschgi, R.; Orvomaa, M.; Belinskij, A.; Keskinen, M. Severe drought in Finland: Modeling effects on water resources and assessing climate change impacts. *Sustainability* **2019**, *11*, 2450. [CrossRef]
23. Lehtonen, I.; Venäläinen, A.; Kämäräinen, M.; Peltola, H.; Gregow, H. Risk of large-scale fires in boreal forests of Finland under changing climate. *Nat. Hazards Earth Syst. Sci.* **2016**, *16*, 239–253. [CrossRef]
24. Adigüzel, F.; Hu, C.; Chen, E.; Siyavus, A.E.; Elmastas, N.; Ustuner, M.; Kaya, A.Y. Impact of Urban Surfaces on Microclimatic Conditions and Thermal Comfort in Burdur, Türkiye. *Atmosphere* **2024**, *15*, 1375. [CrossRef]
25. Miles, V.; Esau, I.; Miles, M.W. The urban climate of the largest cities of the European Arctic. *Urban Clim.* **2023**, *48*, 101423. [CrossRef]
26. Suomi, J. Extreme temperature differences in the city of Lahti, southern Finland: Intensity, seasonality and environmental drivers. *Weather Clim. Extrem.* **2018**, *19*, 20–28. [CrossRef]
27. Das, M.; Das, A. Assessing the relationship between local climatic zones (LCZs) and land surface temperature (LST)—A case study of Sriniketan-Santiniketan Planning Area (SSPA), West Bengal, India. *Urban Clim.* **2020**, *32*, 100591. [CrossRef]
28. Cilek, M.U.; Cilek, A. Analyses of land surface temperature (LST) variability among local climate zones (LCZs) comparing Landsat-8 and ENVI-met model data. *Sustain. Cities Soc.* **2021**, *69*, 102877. [CrossRef]
29. Tanoori, G.; Soltani, A.; Modiri, A. Machine Learning for Urban Heat Island (UHI) Analysis: Predicting Land Surface Temperature (LST) in Urban Environments. *Urban Clim.* **2024**, *55*, 101962. [CrossRef]
30. Emmanuel, R.; Krüger, E. Urban heat island and its impact on climate change resilience in a shrinking city: The case of Glasgow, UK. *Build. Environ.* **2012**, *53*, 137–149. [CrossRef]
31. Emmanuel, R.; Loconsole, A. Green infrastructure as an adaptation approach to tackling urban overheating in the Glasgow Clyde Valley Region, UK. *Landsc. Urban Plan.* **2015**, *138*, 71–86. [CrossRef]
32. Cui, P.; Xv, D.; Tang, J.; Lu, J.; Wu, Y. Assessing the effects of urban green spaces metrics and spatial structure on LST and carbon sinks in Harbin, a cold region city in China. *Sustain. Cities Soc.* **2024**, *113*, 105659. [CrossRef]
33. Crichton, D. The risk triangle. In *Natural Disaster Management*; Ingleton, J., Ed.; Tudor Rose: Leicester, UK, 1999; pp. 102–103, ISBN 0 9536140 0 X.
34. Rosberg, E.; Virtanen, M. Päijät-Hämeen Ilmastonmuutoksen Sopeutumisen Suunnitelma 2023–2030. *Maakuntahallitus* **2023**, *22*, 2023. Available online: https://paijat-hame.fi/wp-content/uploads/2023/05/220523Ilmastonmuutoksen_sopeutumisen_suunnitelma_2023-2030.pdf (accessed on 14 November 2024).
35. ENVI-met Model Architecture. A Holistic Microclimate Model. 2024. Available online: https://envi-met.info/doku.php?id=intro:modelconept (accessed on 27 December 2024).
36. Bröde, P.; Jendritzky, G.; Fiala, D.; Havenith, G. The Universal Thermal Climate Index UTCI in Operational Use. 2010. Available online: https://hdl.handle.net/2134/6086 (accessed on 14 November 2024).
37. Jendritzky, G.; de Dear, R.; Havenith, G. UTCI—Why Another Therm. Index? *Int. J. Biometeorol.* **2012**, *56*, 421–428. [CrossRef] [PubMed]
38. UTCI Homepage. 2024. Available online: https://utci.org/ (accessed on 26 December 2024).
39. Bröde, P.; Krüger, E.; Rossi, F. Assessment of urban outdoor thermal comfort by the universal thermal climate index UTCI. In Proceedings of the 14th International Conference on Environmental Ergonomics, Nafplio, Greece, 10–15 July 2011.
40. Morabito, M.; Crisci, A.; Messeri, A.; Orlandini, S.; Raschi, A.; Maracchi, G.; Munafò, M. The impact of built-up surfaces on land surface temperatures in Italian urban areas. *Sci. Total Environ.* **2016**, *551–552*, 317–326. [CrossRef] [PubMed]

41. Peng, J.; Jia, J.; Liu, Y.; Li, H.; Wu, J. Seasonal contrast of the dominant factors for spatial distribution of land surface temperature in urban areas. *Remote Sens. Environ.* **2018**, *215*, 255–267. [CrossRef]
42. Tan, J.K.N.; Belcher, R.N.; Tan, H.T.W.; Menz, S.; Schroepfer, T. The urban heat island mitigation potential of vegetation depends on local surface type and shade. *Urban For. Urban Green.* **2021**, *62*, 127128. [CrossRef]
43. Zölch, T.; Rahman, M.A.; Pfleiderer, E.; Wagner, G.; Pauleit, S. Designing public squares with green infrastructure to optimize human thermal comfort. *Build. Environ.* **2019**, *149*, 640–654. [CrossRef]
44. Taleghani, M. The impact of increasing urban surface albedo on outdoor summer thermal comfort within a university campus. *Urban Clim.* **2018**, *24*, 175–184. [CrossRef]
45. Schrijvers, P.J.C.; Jonker, H.J.J.; de Roode, S.R.; Kenjereš, S. The effect of using a high-albedo material on the Universal Temperature Climate Index within a street canyon. *Urban Clim.* **2016**, *17*, 284–303. [CrossRef]

Disclaimer/Publisher's Note: The statements, opinions and data contained in all publications are solely those of the individual author(s) and contributor(s) and not of MDPI and/or the editor(s). MDPI and/or the editor(s) disclaim responsibility for any injury to people or property resulting from any ideas, methods, instructions or products referred to in the content.